

# A steady flow model for quiescent prominences

L. Del Zanna and A.W. Hood

Mathematical Sciences Department, University of St. Andrews, St. Andrews, KY16 9SS, Scotland, UK

Received 18 May 1995 / Accepted 13 October 1995

**Abstract.** The normal polarity prominence model of Hood & Anzer (1990) has been modified to include the effect of a steady flow along the magnetic field lines. We consider two isothermal regions that model the hot corona and the cool prominence, considered as a vertical sheet of dense material with infinite length and height but finite width. The magnetic field, pressure and density are assumed to be exponentially decaying in the vertical direction (the velocity is independent of the height in our model) and equations for the horizontal behaviour are determined. Invariance along the prominence direction is assumed, but the magnetic and velocity vectors retain all their components.

The introduction of a field aligned flow results in the coronal magnetic field no longer being force free and a pressure deficit allows a siphon flow to occur. Substantial coronal velocities are possible but only sub-sonic (and hence in the low plasma  $\beta$  corona sub-Alfvénic) flows are considered and these are consistent with observations.

Finally, we propose a simple model for the steady supply of material into a prominence to balance the observed draining motions.

**Key words:** MHD – Sun: corona – Sun: magnetic fields – Sun: prominences – stars: coronae – stars: magnetic fields

## 1. Introduction

Solar prominences have interested theorists and observers for many decades. There are several problems related to the formation, support and eventual eruption that have still to be fully resolved. Among them there is the question of the source of the prominence mass. Two models have been basically discussed in the literature: one is concerned with the condensation of material from the surrounding corona, whereas for the other the mass source is the below chromosphere, with the material being ejected or siphoned into the prominence. The former hypothesis seemed to be supported also by the observations of a *coronal cavity* in the surroundings of a prominence. However, Saito

& Tandberg-Hanssen (1973) found that the missing mass of the cavity was insufficient to account for the prominence mass. Moreover, the fact that a small number of quiescent prominences contains as much mass as the entire corona (Athay 1976) must also be taken into account.

The siphon mechanism to transfer material from the solar surface into a prescribed gravitational dip in a magnetic coronal arcade, such as described in the classical static model by Kippenhahn & Schlüter (1957) (from now on KS), has been shown to be possible by several authors. The first model is due to Pikel'ner (1971), who studied the 1-D equations for a steady flow in a flux tube with a reasonable energy equation. Uchida (1979) and Ribes & Unno (1980) proposed also stationary models belonging to this class, but in the latter the thermodynamics of the system is not taken into account. Poland & Mariska (1986) showed, in a time dependent numerical model, that a sustained heat release in a loop may give rise to an evaporation from below followed by a thermal instability at the top of the loop and a similar result has been found also by Démoulin & Einaudi (1988). Possibly, both mechanisms are responsible for prominence formation. Wu et al. (1987) have investigated a chromospheric injection process, but have demonstrated, solving numerically the 2-D radiative-conductive MHD equations, that this mechanism alone cannot account for the observed mass. An et al. (1988) have incorporated into this injection model the effects of the shear in the magnetic field lines and of converging motions at the chromospheric level.

In the present paper the problem of a steady supply of material from the solar surface into a quiescent prominence is treated, following the idea by Priest & Smith (1979) who suggested, in a cartoon, how a fully formed prominence could be supplied by material through a siphon mechanism with the prominence acting as a sink of material. They assumed that a Rayleigh-Taylor instability allows the plasma to dribble across the magnetic field lines resulting in a slow, but steady down flow. However, in this paper the possibility of the presence of a steady flow along the field lines from the corona into the prominence will be fully demonstrated by solving the complete set of the ideal MHD equations. The structure of the magnetic arcade will result from the solution, that means that in our model the flow plays an active role and is *not* just super-imposed over a static model, as done by the majority of the other authors.

Send offprint requests to: L. Del Zanna

The sign of the average vertical steady flow observed in prominences is still a controversial subject. Earlier observations reported down flows in the threads of prominences seen at the limb (Dunn 1960; Engvold 1976). When large prominences are observed on the disk as dark filaments, however, the Doppler signals indicate both up and down vertical motion with velocities of the order of  $\pm 6 \text{ km s}^{-1}$  in  $\text{H}\alpha$  (Kubota & Uesugi 1986; Schmieder 1989; You & Engvold 1989), thus generating some confusion in the literature concerning the actual motions in the prominence fine-structure. However, in a recent analysis of old, high-resolution observations of limb prominences, Zirker et al. (1994) show that their measurements are in good agreement with the current Doppler measurements on the disk. Their conclusion is that the motions inside a prominence are rather turbulent and that forces other than gravitational seem to control the velocity field pattern.

Around filaments, the transition zone shows an ascending behaviour with persistent large scale motions of the order of  $5 - 10 \text{ km s}^{-1}$  (Lites et al. 1976; Dere et al. 1986) and horizontal motions of the same order close to the prominence axis, with an inclination of  $\simeq 20^\circ$  and parallel to the magnetic field structure. Both these observational results clearly support the validity of the basic assumptions of our model.

The steady flow model for quiescent prominences proposed in the present paper is a generalization of the static model by Hood & Anzer (1990), from now on referred to as HA. This paper was concerned with normal polarity prominences (i.e. the magnetic field passes through the prominence in the same direction as suggested by the underlying photospheric field), like in the classic KS model, but the dipped magnetic structure inside the prominence was derived together with the overall magnetic behaviour of the surrounding corona in a rigorous and self-consistent manner. Here the main assumption was that the magnetic field and gas pressure could be expressed as

$$B \propto (X(x), Y(x), Z(x))e^{-z/2H}, \quad p \propto P(x)e^{-z/H},$$

both inside and outside the prominence region, where  $H$  is the coronal pressure scale height that, since it depends on the temperature, was taken to be a prescribed function of the horizontal coordinate  $x$ . In our paper these basic assumptions are maintained and the presence of a field-aligned velocity is allowed. This will result to be a function of  $x$  only.

The method of solution adopted for our equations is similar to that of Tsinganos et al. (1993), concerning MHD steady flows in uniform gravity. However, their treatment does not allow for the presence of the  $y$  component of the magnetic and velocity fields and it is fully isothermal. Both these restrictions prevent their solutions from being suitable for modelling flows in prominences. Surlantzis et al. (1994) also treated the same problem in a similar way. They solved the 2-D generalized Grad-Shafranov equation in the low  $\beta$  approximation in an attempt to modelling steady flows in coronal loops. A barotropic relation  $P = P(\rho)$  is assumed in order to eliminate an annoying term in the equation and then the temperature is taken as a function of the field lines. But these two assumptions are in contradiction with any reasonable equation of state.

The paper is structured as follows. In Sect. 2 the basic equations and the assumptions for our model are presented. Section 3 is devoted to the discussion of the results from the numerical integration of our equations for values of the parameters suitable for modelling flows in a realistic quiescent prominence. Finally Sect. 4 discusses a possible simple model for the actual replenishment of a prominence by means of the steady mass flow along the coronal arcade field lines.

## 2. Basic model and governing equations

In this section the mathematical equations for our quiescent prominence model are derived. This will be done in two steps. In the first sub-section the general problem of dynamical MHD equilibria in an isothermal and vertically stratified atmosphere with uniform gravity is discussed, whereas the second sub-section is devoted to the prominence model.

### 2.1. Isothermal MHD equilibria in uniform gravity

The purpose of this sub-section is to present the MHD equations governing a mass flow in an isothermal atmosphere with a uniform vertical gravitational field. Since translational symmetry along one of the horizontal directions will be assumed, the most suitable formalism should be that of the generalized Grad-Shafranov equation. However, in this sub-section only the physical assumptions will be presented and a more detailed analysis, following the correct Grad-Shafranov approach, is given in the Appendix.

Consider an ideal, isothermal plasma in a uniform gravitational field (along the  $z$  axis) with a steady mass flow that, for sake of simplicity, is parallel to the field lines. The steady MHD equations are

$$\nabla \cdot (\rho \mathbf{v}) = 0, \quad (1)$$

$$\rho(\mathbf{v} \cdot \nabla)\mathbf{v} = (1/4\pi)(\nabla \times \mathbf{B}) \times \mathbf{B} - \nabla p - \rho g \mathbf{e}_z, \quad (2)$$

$$\nabla \cdot \mathbf{B} = 0, \quad (3)$$

$$\mathbf{v} \times \mathbf{B} = 0, \quad (4)$$

$$p = c^2 \rho, \quad (5)$$

where  $g$  is the (constant) gravitational acceleration,  $c^2 = \mathcal{RT}/\mu$  is the square of the (constant) sound speed and all the other symbols have their usual meaning.

Following the same approach as in HA, consider the magnetic field and the pressure to be separable respectively in the form

$$\mathbf{B} = B_0(X(kx), Y(kx), Z(kx))e^{-kz}, \quad (6)$$

$$p = (B_0^2/4\pi)P(kx)e^{-2kz}, \quad (7)$$

where  $k^{-1}$  is a characteristic length of the system and  $B_0$  is a constant with the dimension of magnetic field. Under these

assumptions, the MHD equations (1) to (5) lead to the following form for the velocity field

$$\mathbf{v} = c \lambda \frac{X}{P}(X, Y, Z), \quad (8)$$

therefore  $\mathbf{v}$  results to be independent from  $z$  in this model, and to the relations

$$Y(kx) = \alpha X / (1 - \lambda^2 X^2 / P), \quad Z(kx) = X', \quad (9)$$

where  $\lambda$  and  $\alpha$  are two dimensionless parameters of the model. After some lengthy calculations, Eq. (2) yields

$$Z' = \frac{\gamma P - X^2 - Y^2 + (1+q)M_A^2 Z^2}{X(1 - M_A^2)}, \quad (10)$$

$$P' = -qPZ/X, \quad (11)$$

where the function  $q$  has been defined as

$$q = \frac{\gamma + M^2 - 2M_A^6/\lambda^2}{1 - M^2 - M_A^2 + M_A^6/\lambda^2}. \quad (12)$$

In these equations,  $\gamma = 2[1/(2kH) - 1]$  is another dimensionless parameter ( $H = c^2/g = \mathcal{R}T/\mu g$  is the pressure scale height), whereas  $M$  and  $M_A$  are respectively the Mach and Alfvénic Mach numbers, given by

$$M^2 = \lambda^2 \frac{X^2}{P^2}(X^2 + Y^2 + Z^2), \quad (13)$$

$$M_A^2 = \lambda^2 X^2 / P = M^2 \beta / 2. \quad (14)$$

Here  $\beta$  is the plasma beta, defined as usual as the ratio of the kinetic and magnetic pressures  $p$  and  $p_m = |\mathbf{B}|^2/8\pi$ , that with our assumptions becomes

$$\beta = 2P/(X^2 + Y^2 + Z^2). \quad (15)$$

Equation (12) simply reduces to  $q = \gamma$  in the static case  $\lambda = 0$  (the term  $2M_A^6/\lambda^2$  is proportional to  $\lambda^4$ ). Note that this result is exactly the same as in Tsinganos et al. (1993), but its validity has been extended here to the more general case  $B_y \neq 0$  and  $v_y \neq 0$ . Needless to say, in the dynamic case  $\lambda \neq 0$ , the equations (10) and (11) must be solved numerically, whatever the value of  $\gamma$ . This is a simple initial value problem for the set of unknown functions  $P(kx)$ ,  $X(kx)$  and  $Z(kx)$ , for any given values of the parameters  $\gamma$ ,  $\alpha$  and  $\lambda$ .

For the general discussion above the critical points of the equations and the solution topologies in the two-dimensional case the reader is referred to Tsinganos et al. (1993). In the present paper the analysis will be restricted to sub-sonic and sub-Alfvénic flows (for which  $q$  and  $Z'$  are always defined), since the goal of our treatment is the investigation of the corrections to the static case due to the introduction of a flow.

## 2.2. The prominence solution

In our attempt to build a prominence model, consider a vertical sheet of cool material of infinite height and length but finite width, surrounded by the hot coronal region. The main assumption in the HA model consists in considering both the prominence and the surrounding corona as isothermal regions with different constant temperatures, namely  $T_{\text{cool}}$  and  $T_{\text{hot}}$ , with  $T_{\text{cool}} \ll T_{\text{hot}}$ . The transition zone between these two regions is then assumed to be so narrow that, taking as plane of symmetry the  $y - z$  plane and considering for simplicity only the region  $x > 0$ , the scale height profile can be assumed to be

$$H(x) = \begin{cases} H_{\text{cool}}, & 0 < x < x_{\text{prom}} \\ H_{\text{hot}}, & x > x_{\text{prom}}, \end{cases} \quad (16)$$

where  $x_{\text{prom}}$  is the prominence half width and where  $H_{\text{cool}} = \mathcal{R}T_{\text{cool}}/\mu_{\text{cool}}g$ ,  $H_{\text{hot}} = \mathcal{R}T_{\text{hot}}/\mu_{\text{hot}}g$ . As in HA, the value  $2H_{\text{hot}}$  is assumed here for the characteristic length  $k^{-1}$ .

In the present model we consider a flow aligned with the magnetic field lines that, starting from one of the foot points of the magnetic arcade, travels across the coronal region, enters the prominence at  $x = x_{\text{prom}}$  and then exits from the other side, ending in the symmetric foot point of the arcade. The presence of the flow modifies the matching conditions for the physical quantities at the interface  $x = x_{\text{prom}}$ , as well as at the symmetric point  $x = -x_{\text{prom}}$ , as follows:

$$[B_x] = 0, \quad (17)$$

$$[\rho v_x] = 0, \quad (18)$$

$$[\rho v_x^2 + p + (1/8\pi)(B_y^2 + B_z^2 - B_x^2)] = 0, \quad (19)$$

$$[\rho v_x v_y - (1/4\pi)B_x B_y] = 0, \quad (20)$$

$$[\rho v_x v_z - (1/4\pi)B_x B_z] = 0, \quad (21)$$

where  $[f]$  is the difference of the values of  $f$  in the two regions at the interface, that is

$$[f] = \lim_{\epsilon \rightarrow 0} [f(x_{\text{prom}} + \epsilon) - f(x_{\text{prom}} - \epsilon)].$$

These are essentially the jump conditions for a MHD oblique shock with  $\mathbf{v} \parallel \mathbf{B}$  (see, for example, Priest 1982). Assuming that the expressions for the physical quantities  $p$ ,  $\rho$ ,  $\mathbf{B}$  and  $\mathbf{v}$  given in the previous sub-section are the same in the two regions, with the same values of  $B_0$  and  $k$  in Eq. (6), relations (17), (20) and (21) imply respectively

$$[X] = 0, \quad (22)$$

$$[(1 - \lambda^2 X^2 / P)Y] = 0, \quad (23)$$

$$[(1 - \lambda^2 X^2 / P)Z] = 0. \quad (24)$$

From Eqs. (18) and (23) the matching conditions for the parameters  $\lambda$  and  $\alpha$  are derived, namely

$$\lambda_{\text{hot}} = \lambda_{\text{cool}} / \sqrt{2kH_{\text{cool}}}, \quad \alpha_{\text{hot}} = \alpha_{\text{cool}}$$

where  $2kH_{\text{cool}} = H_{\text{cool}}/H_{\text{hot}} \ll 1$ . The condition on the pressure function  $P$  can be obtained from Eq. (19) with the aid of Eqs. (22) – (24):

$$[P + \lambda^2 X^4/P] + a^2[(1 - \lambda^2 X^2/P)^{-2}] = 0, \quad (25)$$

where the factor  $a^2 = (1 - \lambda^2 X^2/P)^2(Y^2 + Z^2)/2$  is continuous. This is a non-linear algebraic equation for the value of  $P$  after the discontinuity and it has to be solved numerically. As it will be shown in Sect. 3.1, there is a maximum value for  $\lambda$  beyond which no solution of Eq. (25) can be found. Note that in the static case  $\lambda = 0$  the jump conditions (22) to (25) lead to the continuity of the four functions  $X, Y, Z$  and  $P$ , as expected.

In the prominence and coronal isothermal regions the theory developed in the preceding sub-section is applied. Therefore, the numerical integration starts from the centre of the prominence  $x = 0$  and goes on with  $H = H_{\text{cool}}$  and  $\gamma = 2(H_{\text{hot}}/H_{\text{cool}} - 1) \gg 1$  until  $x_{\text{prom}}$ . Then the jump conditions (22) to (25) are applied and the new initial values and parameters are derived. In the corona  $kH = 1/2$ ,  $\gamma = 0$  and the integration is continued until  $x_{\text{edge}}$ , the foot point of the arcade where  $B_x = 0$  ( $X = 0$ ). Note that in the dynamic case, even if  $\gamma = 0$ , the function  $q$  in Eqs. (10) and (11) is not zero and no analytic solution can be found. Hence the solutions (2.15) in HA for a force free, constant  $\alpha$ -type coronal field with constant pressure in the horizontal direction do not apply in the dynamic case. Deviations from this solution will be analysed in the next section.

The initial values for our model are  $X(0) = X_0$ ,  $Z(0) = Z_0$  and  $P(0) = P_0$ . In order to obtain a solution for which the field lines show a central dip, supporting the dense material of the prominence against gravity, the conditions  $X(0) = 1$ ,  $X'(0) = 0$ ,  $X''(0) > 0$  are assumed, thus  $X_0 = 1$ ,  $Z_0 = 0$  and

$$\beta_0 \equiv 2P_0/(1 + Y_0^2) > 2/\gamma_{\text{cool}} \simeq H_{\text{cool}}/H_{\text{hot}},$$

where  $Y_0 \equiv Y(0) = \alpha_{\text{cool}}/(1 - \lambda_{\text{cool}}^2/P_0)$ . This means that, given the scale heights ratio, the central pressure (or density) cannot be too small while the magnetic field component along the prominence cannot be too large in respect of the normal component. Moreover, other two quantities are required to derive the values of  $\alpha_{\text{cool}}$  and  $\lambda_{\text{cool}}$ . Suitable choices are  $Y_0$  and  $M_0$ , and the other parameters are given by:

$$\lambda_{\text{cool}} = M_0 P_0 / (1 + Y_0^2)^{1/2}$$

$$\alpha_{\text{cool}} = Y_0 [1 - M_0^2 P_0 / (1 + Y_0^2)].$$

Concluding, the parameters that can be selected in our prominence model are five, namely half of the scale heights ratio  $kH_{\text{cool}}$ , which yields the value of  $\gamma$ , the dimensionless prominence half width  $kx_{\text{prom}}$ , the central pressure  $P_0$  in units of  $B_0^2/4\pi$  (for  $z = 0$ ), the magnetic field component  $Y_0$  along the prominence calculated at the origin  $x = 0, z = 0$  and finally the Mach number  $M_0$  at the centre of prominence.

### 3. Results

As values of the parameters of our model we choose the same as in HA, so that the limit to the static case may be easily

checked in order to compare the results. Therefore we take, for the prominence region, the temperature and the mean molecular weight respectively as  $T_{\text{cool}} = 6 \times 10^3$  K and  $\mu_{\text{cool}} = 1$ , giving a pressure scale height  $H_{\text{cool}} = 180$  km. The normal and longitudinal field components at  $x = 0, z = 0$  as  $B_x = 5$  G and  $B_y = 12$  G, yielding  $B_0 = 5$  G and  $\alpha_{\text{cool}} = 2.4$  (in the limit  $\lambda_{\text{cool}} = 0$ ), with a correspondent angle of  $\theta \simeq 22.6^\circ$  between the field and the prominence. The average number density is taken to be  $\bar{n}_{\text{cool}} = 2 \times 10^{17} \text{ m}^{-3}$ ; considering this value as the half of the central density, we take the central pressure as  $p(0, 0) = 2k_B T_{\text{cool}} \bar{n}_{\text{cool}} = 0.0332$  pascals, to be nondimensionalized against  $B_0^2/4\pi \simeq 0.2$  pascals. The width of the prominence is  $2x_{\text{prom}} = 3000$  km. In the corona we choose  $T_{\text{hot}} = 10^6$  K and  $\mu_{\text{hot}} = 0.5$ , with a correspondent scale height of  $H_{\text{hot}} = 6 \times 10^4$  km, so that  $k^{-1} = 1.2 \times 10^5$  km.

The values of the parameters for our model are then

$$kH_{\text{cool}} = 0.0015, \quad kx_{\text{prom}} = 0.0125, \quad P_0 = 0.167, \quad Y_0 = 2.4,$$

that is exactly the same as in HA, to which a value for  $M_0$  has to be added in order to fix the velocity field magnitude. The equations are integrated for four different values of  $M_0$ , namely

$$M_0 = (0.0, 0.5, 0.8, 1.0) \times 10^{-3},$$

and the results are shown in Figs. 1 and 2.

In Figs. 1a and 1b the projections of the magnetic and velocity field lines onto a vertical plane normal to the prominence are shown for a selection of equally spaced  $\xi$ -values, both inside the prominence and for the overall arcade (with different scales). Inside the prominence the field lines exhibit the classical KS structure with  $X$  almost constant. The general behaviour is of the classical support of the dense prominence against gravity provided by the magnetic tension due to the central dip. The half width of the coronal arcade is  $x_{\text{edge}} \simeq 1.4 H_{\text{hot}}$ . Figs. 1c and 1d show the behaviour of the function  $Z(kx)$ , again inside the prominence and for the overall arcade. The rapid turn round of  $B_z$  at  $x = x_{\text{prom}}$  indicates the presence of a strong current flowing inside the prominence, suggesting that the current sheet models are a reasonable approximation. In Fig. 1e we show the modulus of the magnetic field in units of  $B_0$  and for  $z = 0$  inside the prominence as a function of  $kx$ . In Fig. 1f the relative change in the same quantity, with respect to its static constant value, is shown for the four chosen values of the initial Mach number  $M_0$  (in units of  $10^{-3}$ ).

In Fig. 2 the pressure  $P$  (in units  $B_0^2/4\pi$  and for  $z = 0$ ), the Mach number  $M$  and the Alfvénic Mach number  $M_A$  are shown, as functions of  $kx$ , both in the prominence and in the coronal regions. The prominence pressure (Fig. 2a) is unaffected by the flow, while in the corona (Fig. 2b) substantial percentage changes of  $\approx 25\%$  can be found. It is easily seen that only in the static case the pressure is continuous at  $x = x_{\text{prom}}$ , according to Eq. (25). Note that the final pressure at  $x = x_{\text{edge}}$  depends on the strength of the flow. The density  $\rho$  and the plasma  $\beta$ , as  $|\mathbf{B}| \simeq \text{const}$ , behave like the pressure in the two regions but the density show a discontinuity of  $(2kH_{\text{cool}})^{-1} \ll 1$  at  $x_{\text{prom}}$ , entering the corona, due to the jump in the sound speed  $c$ . Also the two Mach

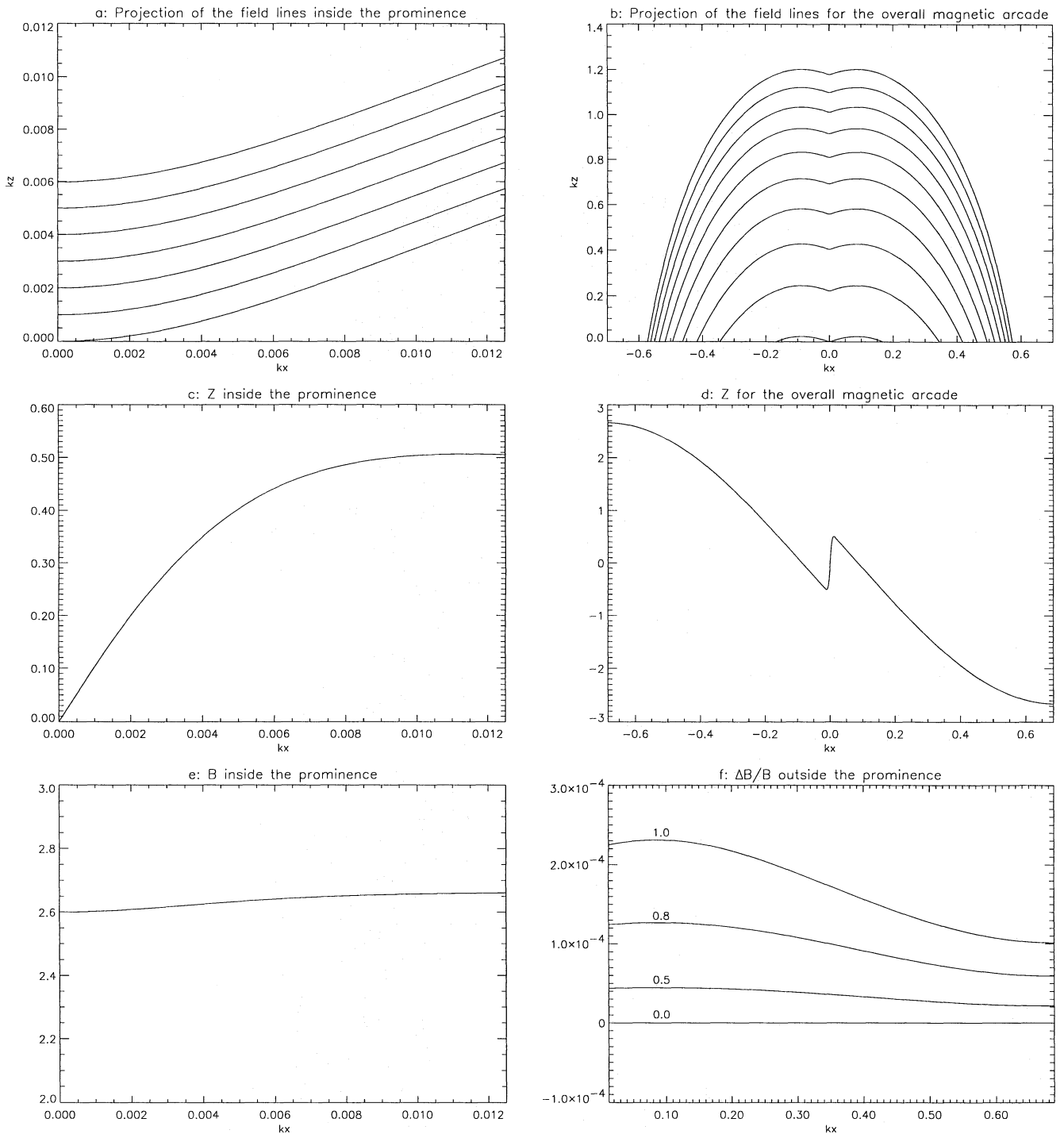


**Fig. 1.** **a** Projection of the magnetic and velocity field lines inside the prominence on a plane normal to the prominence direction. A selection of equally spaced  $\xi$ -values is shown. **b** Projection of the overall arcade for equally spaced  $\xi$ -values, different from **a**. **c** The function  $Z(kx)$  inside the prominence, that is the  $z$ -component of the magnetic field in units of  $B_0$  and for  $z = 0$ . **d** The function  $Z(kx)$  for the overall arcade. **e** Modulus of the magnetic field in units of  $B_0$  and for  $z = 0$  inside the prominence. **f** Relative change in the modulus of the magnetic field, in respect to the static case, for  $z = 0$ . The reference numbers are the values of  $M_0$  in units of  $10^{-3}$

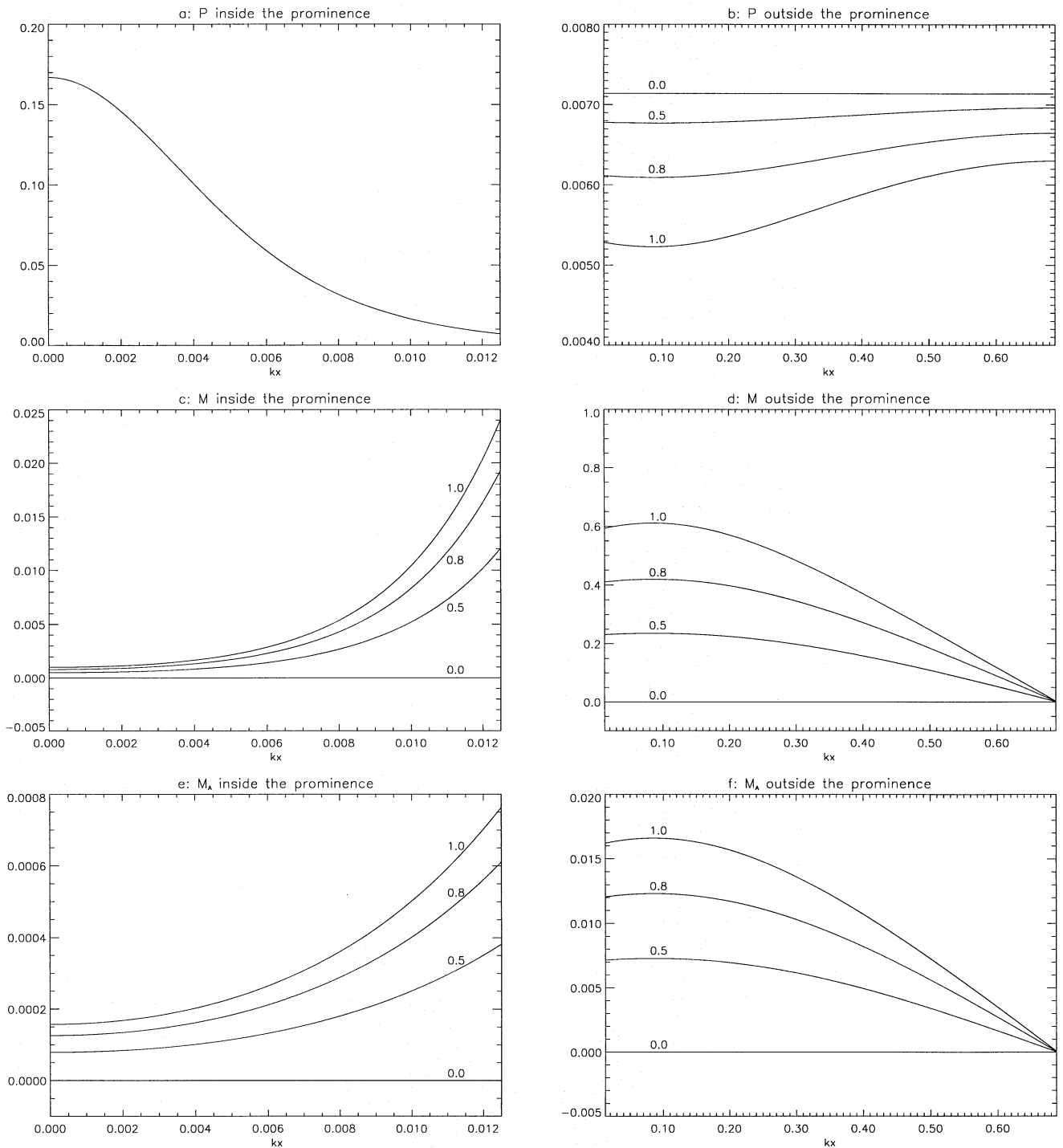


**Fig. 2.** **a** The function  $P(kx)$  inside the prominence, that is the pressure in units of  $B_0^2/4\pi$  and for  $z = 0$ . **b** The function  $P(kx)$  outside the prominence. The meaning of the reference numbers is the same as in Fig. 1f. **c** The Mach number  $M(kx)$  inside the prominence. **d** The Mach number  $M(kx)$  outside the prominence. **e** The Alfvénic Mach number  $M_A(kx)$  inside the prominence. **f** The Alfvénic Mach number  $M_A(kx)$  outside the prominence

numbers are discontinuous functions of  $kx$  at  $x = x_{\text{prom}}$  and the flow is the strongest in the corona. Note that the flow is always sub-sonic and sub-Alfvénic, but in the corona velocities of the same order as the sound speed are allowed. For comparison, the sound speed in the prominence is  $c_{\text{cool}} = \sqrt{gH_{\text{cool}}} \simeq 7 \text{ km s}^{-1}$  and in the corona  $c_{\text{hot}} = \sqrt{gH_{\text{hot}}} \simeq 130 \text{ km s}^{-1}$ . Therefore, if in the prominence region the magnitude of the flow is in the range  $1 - 10^2 \text{ m s}^{-1}$ , that is essentially a static situation, in the corona velocities as high as  $\simeq 100 \text{ km s}^{-1}$  can be reached. This is the reason why the pressure and the magnetic field are unaffected by the flow inside the prominence but may differ from the static case in the corona. This is even clearer in Figs. 2e and 2f, where the Alfvénic Mach number  $M_A$  is plotted for the two regions. Inside the prominence we have  $M_A^2 \simeq 10^{-7}$  and outside  $M_A^2 \simeq 10^{-4}$ . This means that in both cases  $M_A^2 \ll 1$ , so that the factor  $1 - M_A^2$  can be taken as 1 in all the relations where it appears, namely the definition of  $Y$  in Eq. (9), the equation (10) for  $Z'$  and the jump conditions (23) and (24) for  $Y$  and  $Z$ .

Concluding, the prominence region can be considered as static, as the magnetic field and the pressure are not modified by the flow because of the small Mach number and the negligible Alfvénic Mach number. In the corona, the magnetic field is again almost unperturbed by the flow, as the changes in its modulus  $|B|$  and in the angle  $\theta = \cot^{-1}(Y/X)$  between the prominence and the horizontal magnetic field, as well as in the jumps of both the functions  $Y$  and  $Z$  at  $x_{\text{prom}}$ , have a maximum magnitude of approximately  $10^{-4}$ . On the contrary the presence of the flow substantially modifies the pressure. The result is that, in the corona, even if  $\gamma = 0$ , the pressure is no longer constant and hence the situation is no longer force free. Again, the pressure deficit shown in Fig. 2b does not result in a sensible deviation of the magnetic field from the static situation but, on the other hand, it balances a flow with  $M \lesssim 1$ , according to the Bernoulli equation (A14) with  $\gamma = 0$ .

### 3.1. The jump condition for the pressure and the limit on the initial velocity

As it has been anticipated in Sect. 2.2, the freedom in choosing the values of the initial Mach number  $M_0$ , that is the magnitude of the overall flow, is limited by Eq. (25) which is satisfied only if the flow is not too strong. Condition (25) may be rewritten as follows:

$$f(\bar{P}) \equiv \bar{P} + \lambda_{\text{hot}}^2 X^4 / \bar{P} + a^2 (1 - \lambda_{\text{hot}}^2 X^2 / \bar{P})^{-2} - (P + \lambda_{\text{cool}}^2 X^4 / P + a^2 (1 - \lambda_{\text{cool}}^2 X^2 / P)^{-2}) = 0, \quad (26)$$

where all the quantities are calculated at  $x = x_{\text{prom}}$ ,  $\bar{P}$  in the corona just after the interface and  $P$  in the prominence just before it. In Fig. 3 the function  $f(\bar{P})$  is plotted for the usual values of the parameters and for the four chosen values of  $M_0$ . It is clear that a maximum value of  $M_0$  exists and that for higher values no solutions for the pressure satisfying the jump condition Eq. (26), given by the vertical dotted lines, can be found. The presence of a limiting strength of the flow is not due to our particular model nor to any magnetic effect, but it is a general

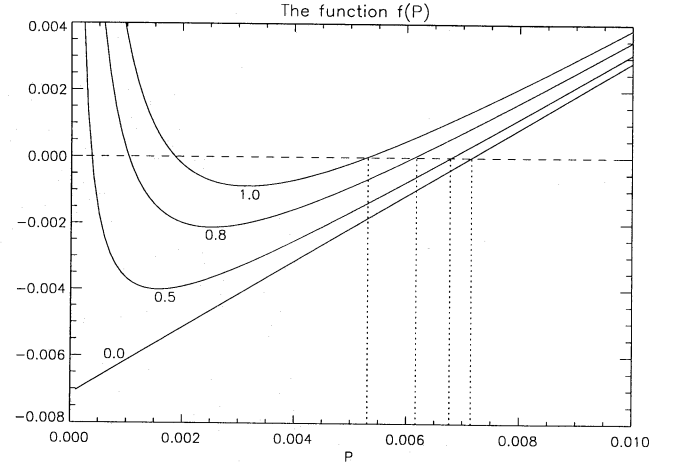


**Fig. 3.** The function  $f(\bar{P})$  defined in Eq. (26), for the usual values of the parameters and for the four chosen values of  $M_0$  (in units of  $10^{-3}$ ). The roots of the equation  $f(\bar{P}) = 0$  are given by the intersections of the curves with the dashed line and these are the values of the pressure  $\bar{P}$  just after the interface  $x = x_{\text{prom}}$ . Note that for too high values of  $M_0$  no solution for  $\bar{P}$  can be found.

hydrodynamic result when considering a flow through an interface between two isothermal regions, where the energy flux is not conserved (see the Appendix). Although the energy equation is different, a very similar situation holds for the *detonation waves*, as described for example in Landau & Lifshitz (1959), where the energy flux is not conserved because of the input of energy due to the combustion of the gas.

A very good approximation of this maximum value  $M_0^{\text{max}}$  of the initial velocity can be obtained easily through an analytic study of Eq. (26) using the approximation  $M_A^2 \ll 1$ . After some straightforward algebra it is easy to see that the function  $f(\bar{P})$  has a minimum for  $\bar{P} = \lambda_{\text{hot}} X \sqrt{X^2 + Y^2 + Z^2}$  and that this minimum must be negative. Then, replacing  $\lambda_{\text{cool}}$  by  $M_0 \beta_0 / 2$  and  $\lambda_{\text{hot}}$  by  $(2kH_{\text{cool}})^{-1/2} M_0 \beta_0 / 2$ , this condition can be written as a quadratic inequality for  $M_0$ . Finally, using the fact that  $2kH_{\text{cool}} \ll 1$ , the solution is

$$M_0 \leq M_0^{\text{max}} \equiv \sqrt{2kH_{\text{cool}}} \frac{\beta/\beta_0}{2X}. \quad (27)$$

It is worth analysing in some detail the dependence of  $M_0^{\text{max}}$  on the different parameters of our model. Throughout the whole prominence, as in the classic KS model,  $X \simeq X_0 = 1$ . Therefore, the only factor that needs to be studied is  $\beta/\beta_0$ , taken at the edge of the prominence region. It is obvious that the influence of  $M_0$  is negligible, as  $\beta/\beta_0$  is calculated inside the prominence; besides, also the initial values  $P_0$  and  $Y_0$  do not affect the behaviour of  $M_0^{\text{max}}$  very much, as  $\beta$  is normalized against  $\beta_0 \equiv 2P_0/(1 + Y_0^2)$  ( $M_0^{\text{max}}(P_0)$  is a decreasing function while  $M_0^{\text{max}}(Y_0)$  is slowly increasing). Hence the two most important parameters are  $kx_{\text{prom}}$  and  $kH_{\text{cool}}$ . The functional form of  $\beta(kx_{\text{prom}})$  is, as a matter of fact, the same as  $P$  shown in Fig. 2a, as the modulus of the magnetic field is almost constant

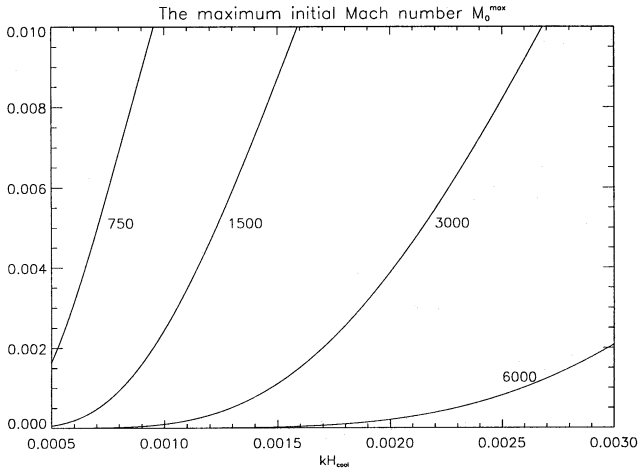


**Fig. 4.** The dependence of the maximum initial Mach number  $M_0^{\max}$ , defined in Eq. (27), by  $kH_{\text{cool}}$  is shown for four values of the parameter  $kx_{\text{prom}}$ , corresponding to the values of the total width of the prominence printed in the picture.

towards the edge of the prominence (Fig. 1e). This means that  $\beta/\beta_0$ , as well as  $M_0^{\max}$ , must be a decreasing function of the width of the prominence. On the other hand, if the temperature difference between the two regions is enhanced, that means increasing  $\gamma_{\text{cool}}$  and decreasing  $kH_{\text{cool}}$ , then again the plasma  $\beta$  decreases because gravity becomes more important inside the prominence and so the pressure falls off faster. The actual behaviour of  $M_0^{\max}$  as a function of  $kH_{\text{cool}}$  and  $kx_{\text{prom}}$  is shown in Fig. 4.

### 3.2. An analytic solution for the low $\beta$ corona

We have seen that the results of our model agree with the observations of a low  $\beta$  coronal plasma, since its maximum value is  $\beta \simeq 0.002$ . Using the fact that  $\beta \ll 1$  it is possible to derive a zeroth order analytic solution as has been done in Tsinganos et al. (1993) in the 2-D case.

From Eq. (14) it is clear that  $\beta \ll 1$  implies  $M_A^2 \ll M^2$ , so that the function  $q$  defined in Eq. (12) reduces to  $q = \frac{M^2}{1-M^2}$ , as  $\gamma = 0$ . Using the relations in Sect. 2.1, the following expressions for the Mach numbers are found:

$$\frac{M}{M_m} e^{-(M^2 - M_m^2)/2} = \frac{X}{X_m}, \quad (28)$$

$$\frac{M_A^2}{M_{A_m}^2} = \frac{X}{X_m} \frac{M}{M_m}, \quad (29)$$

where  $X_m$ ,  $M_m$  and  $M_A$  are the maximum values of the respective functions assumed at the same point  $kx_m$ .

Finally, combining the definitions of  $M^2$  and  $M_A^2$  with Eq. (29) yields

$$\frac{X'^2}{X^2} = \lambda_{\text{hot}}^2 \frac{M^2}{M_A^2} - (1 + \alpha^2) = (1 + \alpha^2) \left[ \frac{X^2}{X_m^2} - 1 \right],$$

with the solution

$$X(kx) = X_m \cos [\sqrt{1 + \alpha^2} k (x - x_m)] \quad (30)$$

for a static, constant  $\alpha$ -type, force free field (e.g. Priest 1982). Thus, the fact that in the corona the presence of a field aligned flow does not affect the shape of the magnetic arcade has been analytically demonstrated under the realistic assumptions of small  $\beta$  and Alfvénic Mach number values. However, the situation is still dynamic and the values of the Mach and Alfvénic Mach numbers are given by Eqs. (28) and (29) respectively, in perfect agreement with the plots in Figs. 2d and 2f.

### 4. A simple model for the prominence mass supply

The main purpose of this paper is to demonstrate the actual possibility of the presence of a flow along the field lines of the whole magnetic arcade, both inside and outside the prominence, studying in detail the jump conditions at the interfaces between the two regions. We have assumed that the mass flow starts from one of the foot points, crosses the narrow prominence region and then falls again down to the solar surface at the other foot point of the same field line.

However, now we want to investigate a symmetric converging flow into the prominence, as suggested, in a simple cartoon, by Priest & Smith (1979) as a possible explanation for the steady replenishment of the prominence mass. As neither the governing equations of our model nor the matching conditions at the interfaces between the prominence and the corona depend on the actual direction of the flow, the only problem to solve is basically the question of the mass conservation inside the prominence. Again, following the idea by Priest & Smith (1979), we assume that the material sucked into the prominence neutralizes cooling down and then dribbles down to the solar surface.

Using the relations derived for our model, it is possible to calculate characteristic quantities like the time scale  $\tau$  of the replenishment process and the down flow velocity, simply derived by imposing the conservation of the total mass of the prominence. Consider a prominence with a finite height extending from  $z = 0$  to  $z = z_{\text{prom}} = 50\,000$  km. The mass and the mass entering per unit time, as functions of  $z$  and per unit length, are respectively given by  $2 \int_0^{x_{\text{prom}}} \int_0^z \rho dx dz$  and  $2 \int_0^z (\rho v_x)_{x_{\text{prom}}} dz$ , yielding

$$m(z) \simeq \frac{B_0^2 P_0 x_{\text{prom}}}{8\pi k c_{\text{cool}}^2} (1 - e^{-2kz}) \quad (31)$$

and

$$\dot{m}(z) \simeq \frac{B_0^2 M_0 P_0}{4\pi k c_{\text{cool}} \sqrt{1 + Y_0^2}} (1 - e^{-2kz}), \quad (32)$$

where we have approximated  $\int_0^{x_{\text{prom}}} P dx \simeq (1/2) P_0 x_{\text{prom}}$  and  $X(kx_{\text{prom}}) \simeq 1$ . The characteristic time scale  $\tau$  is independent of the height:

$$\tau = \frac{m}{\dot{m}} \simeq \frac{x_{\text{prom}} \sqrt{1 + Y_0^2}}{2c_{\text{cool}} M_0}. \quad (33)$$



With the values of the parameters given in Sect. 3 and choosing  $M_0 = 10^{-3}$  we find  $\tau \simeq 6.4$  days. Since the largest initial Mach number has been chosen, the time scale can be greater, in good agreement with the observed average life time of quiescent prominences ( $\simeq 1$  month). Therefore, this result leads to the suggestion that the existence of a quiescent prominence can be explained by a supply of chromospheric material siphoned into the prominence along the magnetic arcade field lines. Once this replenishment ends the prominence might disappear in a slow down flow towards the solar surface. Obviously, the possibility of a final eruption is not taken into account in this simple model.

The down flow speed  $\dot{m}(z)/2 \int_0^{x_{\text{prom}}} \rho dx$  is a function of  $z$ :

$$v_d(z) \simeq \frac{c_{\text{cool}} M_0}{k x_{\text{prom}} \sqrt{1 + Y_0^2}} [1 - e^{-2k(z_{\text{prom}} - z)}], \quad (34)$$

and the maximum velocity, at the bottom end of the prominence, is  $v_d \simeq 0.12 \text{ km s}^{-1}$ . This value is rather small and confirms the result of an almost static situation inside the prominence region ( $v_d$  has the same order of magnitude of the entering velocity, as may be seen in Fig. 2c).

## 5. Conclusions

In this paper the problem of steady flows in quiescent prominences has been treated. The prominence has been considered as a vertical cool sheet with finite length embedded in the surrounding hot corona. The magnetic field and gas pressure have been assumed to be separable in the horizontal and vertical coordinates and an exponentially decaying behaviour has been chosen for the latter. These assumptions are the same as in the static HA model, so that our treatment may be considered as dynamical extension to the static case.

Both the prominence and coronal regions have been regarded as isothermal (with different temperatures) and, in each region, the generalized Grad-Shafranov equation for an isothermal, steady, MHD flow in uniform gravity has been solved. The method used is similar to that of Tsinganos et al. (1993), but here the vector fields retain all their components. The equations have been solved numerically and without the need of any approximation. The two solutions have been then matched solving the set of jump conditions at the boundary surfaces between the two isothermal regions. Since the energy flux is not conserved crossing these surfaces, a limiting strength for the flow has been found and this makes the flow always sub-sonic (and sub-Alfvénic as the plasma  $\beta$  is small everywhere).

The results are that the static magnetic configuration is slightly affected by the presence of the flow only in the coronal region, while the structure inside the prominence (that exhibits the classic KS dip for the magnetic support against gravity) can be still considered as static. On the other hand, the coronal pressure shows a deficit allowing the flow to occur and therefore the configuration is no longer force free as in the static case. The average velocities in the corona are of the order of  $50 \text{ km s}^{-1}$ , in good agreement with the observations, whereas inside the prominence  $v \lesssim 0.1 \text{ km s}^{-1}$ .

Finally, the suggestion by Priest & Smith (1979) for the mechanism of the prominence mass supply has been revisited using the results of our model. The characteristic time scale of the mass replenishment is of the same order of magnitude as the observed average life time of quiescent prominences, suggesting that their existence is indeed connected to the mass supply from the below chromosphere.

## Appendix A: the Grad-Shafranov formalism

In this Appendix the same results presented in Sect. 2.1 will be derived following the Grad-Shafranov formalism, that is the natural mathematical approach when modelling steady flows with an ignorable spatial coordinate. A complete treatment of this subject may be found in Del Zanna & Chiuderi (1995), where several *exact* solutions are derived for the incompressible case (among them there is an interesting class of arcade-type solutions in uniform gravity in which the flow is not parallel with the magnetic field) and to which the reader is implicitly referred for any mathematical demonstration.

In the present case, consider all the physical quantities to be independent of  $y$  (in cartesian coordinates), that is

$$\partial/\partial y \equiv 0. \quad (A1)$$

The assumption of translational symmetry allows one to write the magnetic and velocity vectors respectively as

$$\mathbf{B} = \dot{A} [\nabla \xi \times \mathbf{e}_y + (\chi/h) \mathbf{e}_y], \quad (A2)$$

$$\mathbf{v} = \dot{\Psi}/4\pi\rho [\nabla \xi \times \mathbf{e}_y + (\chi/h) \mathbf{e}_y], \quad (A3)$$

where  $\xi(x, z)$  is a dimensionless flux function,  $A$ ,  $\Psi$  and  $\chi$  are free functions of  $\xi$  (the dot implies differentiation with respect to  $\xi$ ) and where

$$h(\xi, \rho) = \dot{A}^2 - \dot{\Psi}^2/4\pi\rho. \quad (A4)$$

The surfaces  $\xi = \text{const}$  contain both the magnetic and velocity field lines and all the free functions of  $\xi$  are called *surface functions*.

Using the definitions of all the surface functions, it can be demonstrated that Euler's equation, Eq. (2), becomes

$$h \nabla^2 \xi + \frac{1}{2} \frac{\partial h}{\partial \xi} |\nabla \xi|^2 + 4\pi \left( \frac{\dot{\Psi}}{4\pi\rho} \right)^2 (\nabla \rho \cdot \nabla \xi) + \frac{1}{2} \frac{\partial}{\partial \xi} \left( \frac{\chi^2}{h} \right) + 4\pi\rho \dot{W} = 0, \quad (A5)$$

where the fourth surface function  $W(\xi)$  is defined by

$$c^2 \ln \rho + \frac{1}{2} \left( \frac{\dot{\Psi}}{4\pi\rho} \right)^2 \left[ |\nabla \xi|^2 + \left( \frac{\chi}{h} \right)^2 \right] + gz = W. \quad (A6)$$

Equation (A5) is the *generalized Grad-Shafranov equation* for the flux function  $\xi(x, z)$ , while Eq. (A6) is the *generalized Bernoulli equation* for the density  $\rho(x, z)$  in the isothermal case.

These two nonlinear equations are strongly coupled together, especially through the third term in Eq. (A5), which determines also its mathematical nature.

The same assumptions as in Sect. 2.1 are recovered choosing

$$\xi = X(kx)e^{-kz}, \quad (\text{A7})$$

$$\rho = (B_0^2/4\pi c^2)P(kx)e^{-2kz}, \quad (\text{A8})$$

and the free surface functions as

$$\dot{A}(\xi) = k^{-1}B_0 = \text{const}, \quad (\text{A9})$$

$$\dot{\Psi}(\xi) = \lambda(k^{-1}B_0^2/c)\xi, \quad (\text{A10})$$

$$\chi(\xi) = \alpha(k^{-1}B_0^2)\xi, \quad (\text{A11})$$

$$W(\xi) = c^2 \ln \xi^{-\gamma}, \quad (\text{A12})$$

that also eliminates the  $z$  dependence in the two equations. Note that in the planar case  $\chi = 0$  these functions are the same as in Tsinganos et al. (1993), although the formalism used is slightly different.

Using these definitions it is now possible to rewrite the two governing equations respectively as

$$(1 - M_A^2)XZ' + X^2 + Y^2 - \gamma P -$$

$$M_A^2(1 - XP'/ZP)Z^2 = 0, \quad (\text{A13})$$

$$\gamma \ln(X/X_*) + \ln(P/P_*) + (M^2 - M_*^2)/2 = 0, \quad (\text{A14})$$

where  $X_*$ ,  $P_*$  and  $M_*$  are reference values for  $X$ ,  $P$  and  $M$ , respectively. After some lengthy calculations, involving the derivative of Eq. (A14) in respect of  $kx$ , these lead to Eqs. (10) and (11).

Concluding, it is worth noticing that the jump conditions for the prominence model at the boundary  $x = x_{\text{prom}}$ , Eqs. (17), (18) and (20) in Sect. 2.2, yield directly the continuity of the surface functions  $\dot{A}$ ,  $\dot{\Psi}$  and  $\chi$  defined in Eqs. (A9) to (A11). However, note that the function  $W$  does not have to be continuous since the energy flux is not conserved at the boundary surface  $x = x_{\text{prom}}$  between the two isothermal regions. In fact, the last jump condition for the energy flux reads

$$[W] + \lim_{\epsilon \rightarrow 0} \int_{x_{\text{prom}} - \epsilon}^{x_{\text{prom}} + \epsilon} S \frac{dT}{dx} dx = 0, \quad (\text{A15})$$

where  $S$  is the entropy per unit mass, given by  $S = (\mathcal{R}/\mu)(1 - \ln \rho)$  (Hameiri 1983; Agim & Tataronis 1985). It is clear that, since  $dT/dx$  behaves like a delta function for  $x = x_{\text{prom}}$ , the free function  $W$  must be discontinuous at that point, according to its definition in Eq. (A12). Therefore, the integral in Eq. (A15) simply gives the input of energy necessary to balance the energy flux  $W$  and need not to be evaluated (note that the  $z$  dependence cancels from the two terms  $W$  and  $S$ ).

## References

- Agim Y. Z., Tataronis J. A., 1985, *J. Plasma Phys.* 34(3), 337  
 An C.-H., Wu S. T., Bao J. J., 1988, in: *Proc. Mallorca Workshop on Dynamics and Structure of Solar Prominences*, eds. J. L. Ballester, E. R. Priest  
 Athay R. G., 1976, in: *The Solar Chromosphere and Corona: Quiet Sun*, D. Reidel Publ. Co., Dordrecht, Holland, p. 91  
 Del Zanna L., Chiuderi C., 1995, *A&A* (in press)  
 Démoulin P., Einaudi G., 1988, in: *Proc. Mallorca Workshop on Dynamics and Structure of Solar Prominences*, eds. J. L. Ballester, E. R. Priest  
 Dere K. P., Bartoe J.-D. F., Brueckner G. E., 1986, *ApJ* 310, 456  
 Dunn, R. B., 1960, Ph. D. Thesis, Univ. Harvard  
 Engvold O., 1976, *Solar Phys.* 49, 283  
 Hameiri E., 1983, *Phys. Fluids* 26, 230  
 Hood A. W., Anzer U., 1990, *Solar Phys.* 126, 117  
 Kippenhahn R., Schlüter A., 1957, *Z. Astrophys.* 43, 36  
 Kubota J. Uesugi A., 1986, *Publ. Astron. Soc. Japan* 38, 903  
 Landau L. D., Lifshitz E. M., 1959, in: *Fluid Mechanics*, translated from the Russian by J. B. Sykes, W. H. Reid, Oxford Pergamon Press  
 Lites B. W., Bruner E. C., Chipman E. G., Shine R. A., Rottman G. J., White O. R., Athay R. G., 1976, *ApJ* 210, L111  
 Pikel'ner S. B., 1971, *Solar Phys.* 17, 44  
 Poland A. I., Mariska J. T., 1986, *Solar Phys.* 104, 303  
 Priest E. R., 1982, in: *Solar Magnetohydrodynamics*, D. Reidel Publ. Co., Dordrecht, Holland  
 Priest E. R., Smith E. A., 1979, *Solar Phys.* 64, 217  
 Ribes E., Unno W., 1980, *A&A* 91, 129  
 Saito K., Tandberg-Hanssen E., 1973, *Solar Phys.* 31, 105  
 Schmieder B., 1989, in: *Dynamics of Quiescent Prominences*, Lecture Notes in Physics, eds. V. Ruždjak, E. Tandberg-Hanssen, p. 85  
 Surlantzis G., Démoulin P., Heyvaerts J., Sauty C., 1994, *A&A* 284, 985  
 Tsinganos K., Surlantzis G., Priest E. R., 1993, *A&A* 275, 613  
 Uchida Y., 1979, in: *Proc. of the Japan-France seminar on Solar Phys.*, eds. J. C. Henoux, p. 169  
 Wu S. T., Bao J. J., An C.-H., Tandberg-Hanssen E., 1988, in: *Proc. Mallorca Workshop on Dynamics and Structure of Solar Prominences*, eds. J. L. Ballester, E. R. Priest  
 You, Engvold O., 1989, *Hvar Obs. Bull.* 13, 197  
 Zirker J. B., Engvold O., Yi Z., 1994, *Solar Phys.* 150 (1-2), 81